Hexavalent chromium mobility in a high amorphous phase Chromite Ore Processing Residue (COPR) in the perspective of a chromium remediation treatment

Etude de la mobilité du chrome hexavalent dans la perspective d'une dépollution des charrées de chrome à forte teneur en phases amorphes

Arnaud Sanchez-Hachair[(1*)], Natacha Henry[(2)], Valentin Bastien[(3)], Khadijetou Diakite[(1)], Guillaume Carlier[(3)], Gaëtan Lefebvre[(4)], Céline Hébrard-Labit[(3)], Annette Hofmann[(1*)]

[(1)]Université de Lille, CNRS, Université Littoral Côte d'Opale, UMR 8187, LOG, Laboratoire d'Océanologie et de Géosciences, 59000 Lille, France

[(2)]Université de Lille, CNRS, Centrale Lille, ENSCL, Université Artois, UMR 8181, Unité de Catalyse et Chimie du Solide, 59000 Lille, France

[(3)]CEREMA - Centre d'études et d'expertise sur les risques, l'environnement, la mobilité et l'aménagement, Direction territoriale Nord-Picardie, 59019 Lille, France

[(4)]DIR-Nord – Direction interdépartementale des routes Nord, Service des politiques et techniques, Cellule Ingénierie entretien chaussées dépendances, 59019 Lille, France

*arnaud.sh@live.fr; annette.hofmann@univ-lille.fr

Supplementary information

S1] Formation of Chromite Ore Processing Residue

Chromium is a common heavy metal pollutant in soils, groundwater and industrial waste materials. Indeed, chromium is used industrially since the 19th century, first by westeners (Guertin et al. 2005), and world wide at present time. Chromium is used in metallurgy for the manufacture of stainless steels (90 %), and in chemistry (6 %) for pigments, catalytic agents in organic chemistry (Rase, 2000), tanning agents, wood and metal surfaces protection. The remaining part (4 %) is used for the production of refractory materials for metal furnaces (Blazy and Hermant, 2014). In mining, chromium ranks at the seventh position with a production of 31 million tons in 2017 (U.S. Geological Survey, 2018). The chromite ore is extracted from igneous bedded stratiform rocks and podiform ophiolitic deposits.

The primary material contains:

- Fe-chromite ($FeCr_2O_4$), Mg-chromite ($MgCr_2O_4$) and Mn-chromite ($MnCr_2O_4$), i.e. the main ore minerals. Sometimes metal sulphide inclusions are observed (Melcher et al., 1997).
- Silicates such as olivine ($(Mg,Fe)_2[SiO_4]$), diopside ($CaMgSi_2O_6$), antigorite ($(Mg,Fe)_3Si_2O_5(OH)_4$), enstatite ($Mg_2Si_2O_6$), anorthite ($CaAl_2Si_2O_8$) and minerals from the amphibole group (tremolite $Ca_2Mg_5[Si4O11(OH)]_2$ and actinolite $Ca_2Mg_5Si_8O_{22}(OH)_2$). These minerals are essentially present in poor quality chromite ores.
- Oxides and hydroxides such as hematite (Fe_2O_3), goethite ($FeO(OH)$ and brucite ($Mg(OH)_2$), oxides from the spinel familly (picotite $(Fe,Mg)(Al,Cr)_2O_4$, hercynite $FeAl_2O_4$ and magnetite Fe_3O_4), rutile (TiO_2), and quartz (SiO_2).
- Rarely carbonates (calcite $CaCO_3$ and dolomite $MgCO_3$) (Zubakov and Yusupova, 1962).

For the needs of the chemical industry, a high degree of purity of the chromium extract is requiered. To reach this goal, the ore is treated hydrometallurgically. Chromite minerals contain chromium in the oxidation state +III which is difficult to extract. Therefore Cr(III) is transformed to oxidation state +VI, under which the element is more mobile. To achieve chromium oxidation, the chromite ore is crushed into 2 mm size particles and roasted in a rotative furnace at 1000-1200°C. Sodium carbonate (Na_2CO_3) is added, allowing the formation of sodium chromate (Na_2CrO_4) as shown in equation I.

$$FeCr_2O_4 + 2Na_2CO_3 + \frac{7}{4}O_2 \rightarrow 2Na_2CrO_4 + \frac{1}{2}Fe_2O_3 + 2CO_2 \quad \text{(I)}$$

Lime (CaO) is useful to capture dissolved silicate and avoid the formation of silica gel which slows down the transformation of Cr(III) to Cr(VI). The reaction of lime with silicate leads to the formation of bi and tri-calcium silicate phases (cement terminology: C2S, belite and C3S, alite). Also in the presence of dissolved aluminate, lime can react to form tricalcium aluminate (C3A) and tetra-calcium aluminoferrite phases (C4AF). These phases are precursors of cement phases (le Chatelier, 1919; Lea, 1970; Lothenbach and Winnefeld, 2006). After the roasting step, the chromite ore is leached to extract CrO_4^{2-} and Na^+. The leachate is dessicated to form a pure Na_2CrO_4 salt, ready to use for the synthesis of chemical reagents. The thermo-alkaline oxidation method involved in this extraction method is characterized by low extraction efficiency. Only 30 to 45 % of Cr(III) is transformed to Cr(VI) and only 75 to 90 % of Cr(VI) is extracted from the roasted ore (Deakin et al., 2001). The uncomplete oxidation of chromite is linked to several inhibiting processes. Even if lime is added during the treatment, silica gel can form. Also, in the presence of carbonate, a binary Na_2CO_3-Na_2CrO_4 eutectic solution is formed when chromite is roasted, further preventing the penetration of oxygen necessary for the oxidation reaction (Tathavadkar et al., 2001, 2003). The residual product obtained is called Chromite Ore Processing Residue (COPR). During the cooling of the COPR, the precursors of the cement phases (C3S, C2S, C3A and C4AF) take in water molecules and transform into cement phases as shown in figure S1.

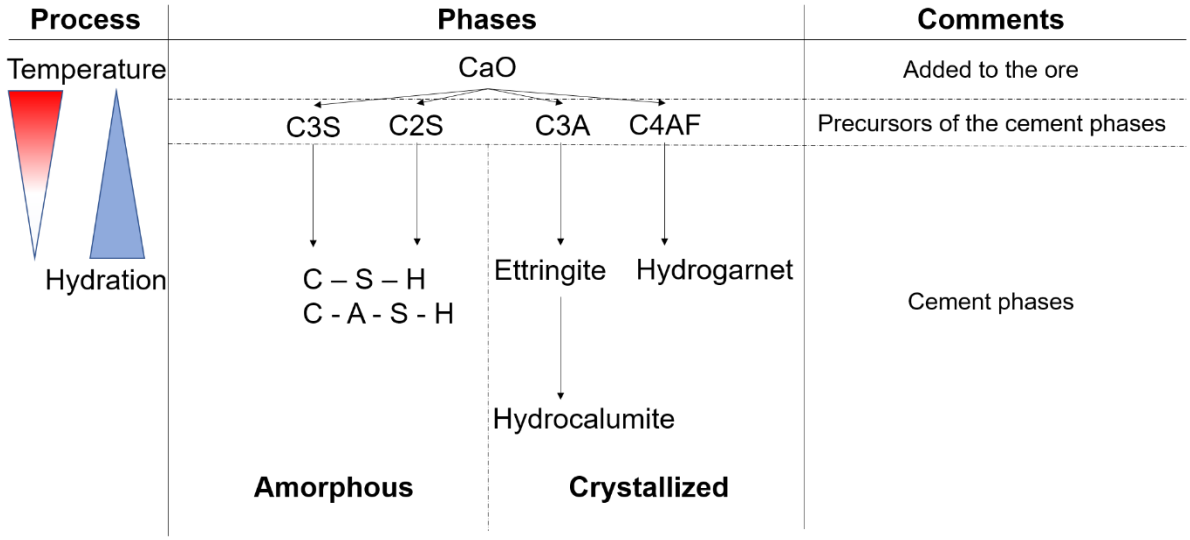

Fig. S1 *Cementitious complexes formed in COPR in the presence of lime and their evolution during hydration and cooling. C3S: tri-calcium silicate (alite); C2S: di-calcium silicate (belite); C3A: tri-calcium aluminate; C4AF: tetra-calcium aluminoferrite (also called brownmillerite); C-S-H: Calcium Silicate Hydrate; C-A-S-H: Calcium Aluminate Silicate Hydrate*

During hydration, C3S and C2S are transformed to amorphous Calcium Silicate Hydrate (C-S-H). Calcium Aluminate Silicate Hydrate (C-A-S-H) phases can also be formed when aluminate is present in the solution. These phases are the most preeminent amorphous phases in cement. On the other hand, C3A and C4AF (also called brownmillerite $Ca_2(Fe,Al,Cr(III))O_5$) are hydrated to the crystalline phases of ettringite (C6AS3Hn: $Ca_6Al_2(SO_4;CrO_4)_3(OH)_{12}.nH2O$ 26<n<34), hydrocalumite (C4AH13: $Ca_4(Al,Fe)_2(OH)_{12}CrO4.6H_2O$) and hydrogarnet (C3AH6 : $Ca_3(Al,Fe)_2(H_4O_4,CrO_4)_3$) (Minard, 2003). These three latter phases can fix oxyanions (SO_4^{2-}, CrO_4^{2-}, AsO_4^{2-}, SeO_4^{2-}, MoO_4^{2-}, VO_4^{3-}) in their structure (Chrysochoou and Dermatas, 2006; Geelhoed et al., 2002; Gougar et al., 1996; Hillier et al., 2003; Kindness et al., 1994; McCarthy et al., 1991; Myneni, 1995). The authors cited here identified several types of uptake phenomena. For ettringite, oxyanion absorption in central channel position and adsorption on the positively charged surfaces are possible (Myneni, 1995; Myneni et al., 1998). Hydrocalumite has a layered double hydroxide (LDH) structure in which oxyanions can be taken up by anion exchange (Chrysochoou and Dermatas, 2006) while the hydrogarnet structure allows oxyanion uptake at tetrahedral surface sites (Hillier et al., 2007). Thus, all these phases can adsorb oxyanions because of positively charged surfaces. Conversely, amorphous cement phases cannot easily adsorb oxyanions because the presence of tetrahedral silicate in their structure induces negative surface charge when CaO is completely consumed (Nonat, 2004).

Bibliography

Blazy, P., Hermant, V., 2014. Métallurgie extractive du chrome. *Tech. Ing. Métallurgie Extr.* ref.article : m2245 base documentaire : TIB369DUO.

Chrysochoou, M., Dermatas, D., 2006. Evaluation of ettringite and hydrocalumite formation for heavy metal immobilization: Literature review and experimental study. *J. Hazard. Mater*. 136:20–33.

Deakin, D., West, L.J., Stewart, D.I., Yardley, B.W.D., 2001. Leaching behaviour of a chromium smelter waste heap. *Waste Manag.* 21:265–270.

Geelhoed, J.S., Meeussen, J.C., Hillier, S., Lumsdon, D.G., Thomas, R.P., Farmer, J.G., Paterson, E., 2002. Identification and geochemical modeling of processes controlling leaching of Cr (VI) and other major elements from chromite ore processing residue. *Geochim. Cosmochim. Acta* 66:3927–3942.

Gougar, M.L.D., Scheetz, B.E., Roy, D.M., 1996. Ettringite and C-S-H Portland cement phases for waste ion immobilization: A review. *Waste Manag.* 16:295–303.

Guertin, J., Jacobs, J.A., Avakian, C.P., 2005. *Chromium(VI) Handbook*. New York.CRC Press.

Hillier, S., Lumsdon, D.G., Brydson, R., Paterson, E., 2007. Hydrogarnet: A host phase for Cr(VI) in Chromite Ore Processing Residue (COPR) and other high pH wastes. *Environ. Sci. Technol.* 41:1921–1927.

Kindness, A., Macias, A., Glasser, F.P., 1994. Immobilization of chromium in cement matrices. *Waste Manag.* 14:3–11.

le Chatelier, H., 1919. Crystalloids against colloids in the theory of cements. *Trans. Faraday Soc.* 14:8–11.

Lea, F.M., 1970. *The chemistry of cement and concrete*. Third edition. London

Lothenbach, B., Winnefeld, F., 2006. Thermodynamic modelling of the hydration of Portland cement. *Cem. Concr. Res.* 36:209–226.
McCarthy, G.J., Hassett, D.J., Bender, J.A., 1991. Synthesis, crystal chemistry and stability of ettringite, a material with potential applications in hazardous waste immobilization. *MRS Proc.* 245.
Melcher, F., Grum, W., Simon, G., Thalhammer, T.V., Stumpfl, E.F., 1997. Petrogenesis of the ophiolitic giant chromite deposits of kempirsai, Kazakhstan: a study of solid and fluid inclusions in chromite. *J. Petrol.* 38:1419–1458.
Minard, H., 2003. Etude intégrée des processus d'hydratation, de coagulation, de rigidification et de prise pour un système C3S-C3A - sulfates - alcalins. Dissertation. Université de Bourgogne, Dijon, France.
Myneni, S.C.B., 1995. Oxyanion mineral surface interact ions in alkaline environments: AsO4 and CrO4 sorption and desorption in ettringite. Dissertation. The Ohio State University, Colombus, US. 265p.
Myneni, S.C.B., Traina, S.J., Logan, T.J., 1998. Ettringite solubility and geochemistry of the Ca(OH)(2)-Al-2(SO4)(3)-H2O system at 1 atm pressure and 298 K. *Chem. Geol.* 148:1–19.
Nonat, A., 2004. The structure and stoichiometry of C-S-H. *Cem. Concr. Res.* 34:1521–1528.
Rase, Howard.F., 2000. *Handbook of commercial catalysts: heterogeneous catalysts.* Taylor & Francis, CRC Press.
Tathavadkar, V.D., Jha, A., Antony, M.P., 2003. The effect of salt-phase composition on the rate of soda-ash roasting of chromite ores. *Metall. Mater. Trans. B* 34:555–563.
Tathavadkar, V.D., Jha, A., Antony, M.P., 2001. The soda-ash roasting of chromite minerals: Kinetics considerations. *Metall. Mater. Trans. B* 32:593–602.
U.S. Geological Survey, 2018. *Mineral commodity summaries 2018*. U.S. Geological Survey.
Zubakov, S.M., Yusupova, E.N., 1962. Composition and properties of chromite ores from new deposits in Kazakhstan. *Refractories* 3:341–344.

S2] Sampling of COPR materials

All COPR materials used in this study were obtained through auger drilling. All drillings were performed within a distance of 1-2 meters from each other on the same site. Drilling PZ2 was performed in 2013. In this test, the COPR material was retrieved from depth 2.5-3 m. Drillings of the T-RX series were performed in 2015, at a location close to PZ2. Two boreholes were set-up at 1 m distance from each other. Figures S2a show s the stratigraphy of deposits at these locations with the position of batches T-RX, T-RX2, T-RX3 and T-RX4 indicated. The XRD traces of the materials in the different layers are given in Fig. S2b.

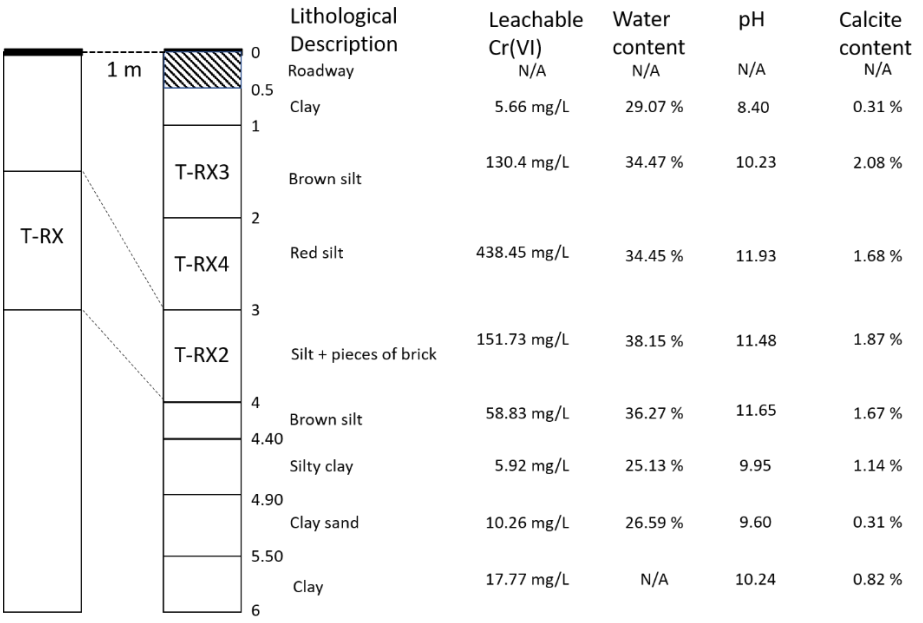

Lithological Description	Leachable Cr(VI)	Water content	pH	Calcite content
Roadway	N/A	N/A	N/A	N/A
Clay	5.66 mg/L	29.07 %	8.40	0.31 %
Brown silt	130.4 mg/L	34.47 %	10.23	2.08 %
Red silt	438.45 mg/L	34.45 %	11.93	1.68 %
Silt + pieces of brick	151.73 mg/L	38.15 %	11.48	1.87 %
Brown silt	58.83 mg/L	36.27 %	11.65	1.67 %
Silty clay	5.92 mg/L	25.13 %	9.95	1.14 %
Clay sand	10.26 mg/L	26.59 %	9.60	0.31 %
Clay	17.77 mg/L	N/A	10.24	0.82 %

Fig S2a *Stratigraphy of the backfill at the location of the drillings. Vertical positions of batches T-RX, T-RX2, T-RX3 and T-RX4. Mean values of chemical and physical data for each layer.*

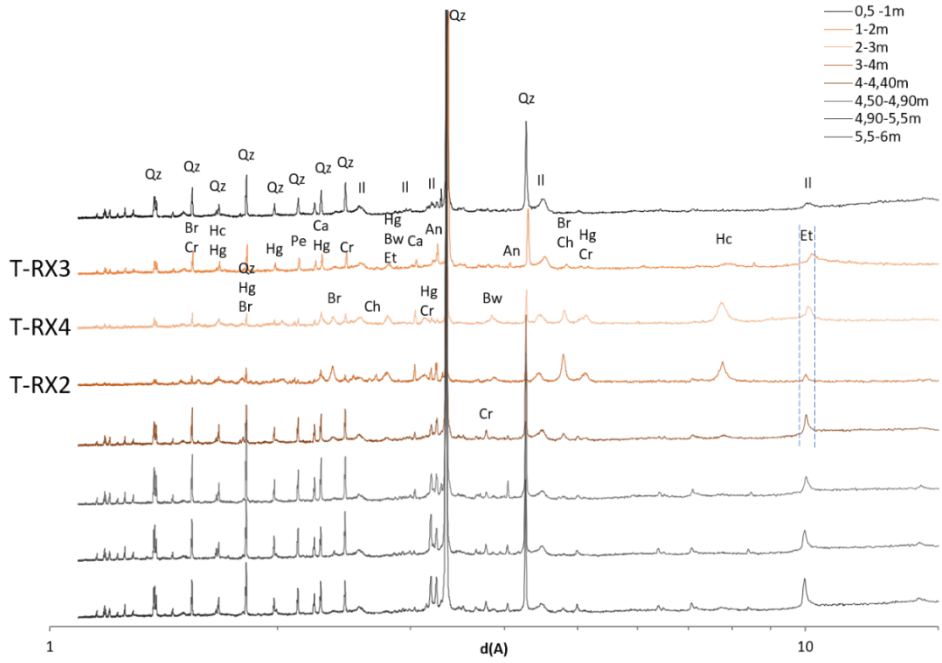

Fig. S2b *X-ray diffractogrammes for each layer in drilling 2 (0,5 to 6 m depth). Annotations : Qz quartz ; Il illite ; Ca calcite ; Et ettringite ;Hc hydrocalumite ; Hg hydrogarnet ; Cr crocoite ; Br brucite ; Ch chromite ; Bw brownmillerite ; Pe periclase ; An anorthite. The black coloured diffractograms correspond to non COPR, those in brown colours correspond to COPR materials.*

S3] XRPD-Rietveld analysis: additional details on methodology

For best quality of the XRPD-Rietveld analysis, samples were prepared thoroughly. Samples were dried (65°C, 48 hours) and then manually crushed in an agate mortar for 15 minutes. This soft mechanical method allowed minimizing the formation of toxic dust particles. The powder was deposited in a XRD sample holder and a perfectly even flat surface was obtained by dense packing of the material and scraping off the surplus with a blade spatula. XRPD patterns were recorded from 3 to 90° 2θ, in steps of 0.0214° and a step-time of 1.75 s. The calculated diffractogram is obtained by combination of pseudo-Voigt functions for each individual mineral phase. We let the software adjust the mathematical settings for Lorentzian and Gaussian shape of peaks. Asymmetry of the diffraction peaks was corrected with the Bérar-Baldinozzi equation (Bérar and Baldinozzi, 1993). Shutoff parameters were the number of calculation cycles to reach unit cell parameters (20) and a convergence criterion of 0,05 for parameter values of two consecutive cycles.

Bibliography

Bérar, J.-F., Baldinozzi, G., 1993. Modeling of line-shape asymmetry in powder diffraction. *J. Appl. Crystallogr*. 26:128–129.

S4] Appearance of quartz particles in SEM-images

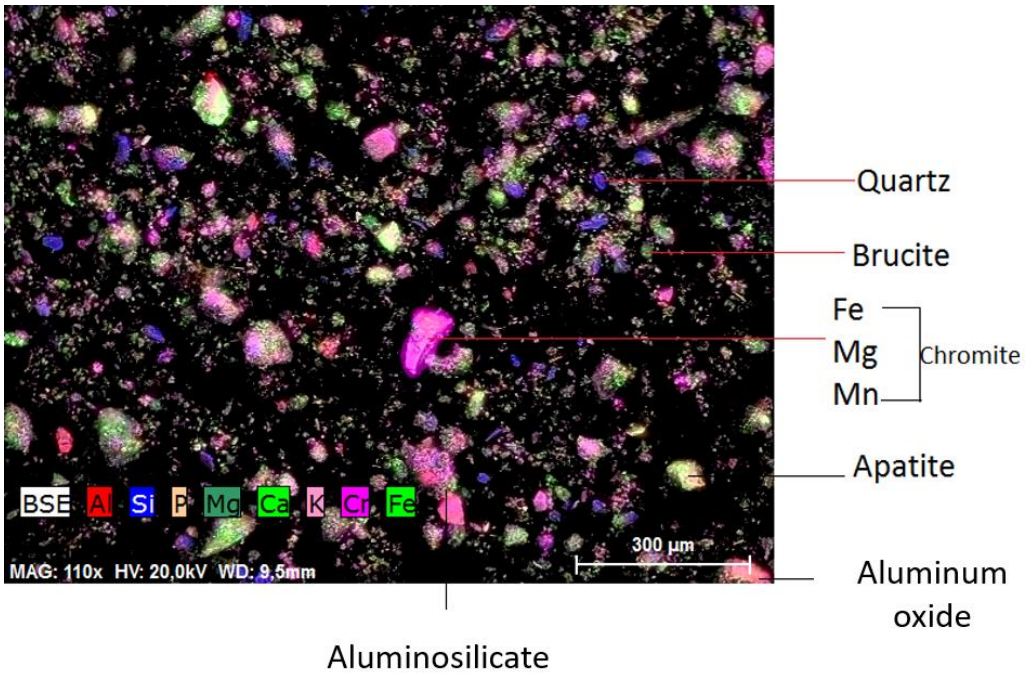

Fig. S4a *Scanning electron microscopy image in backscattering mode and elemental map by EDS analysis on a dry sample of batch T-RX2 sieved between 15 – 100 um size. Mineral attributions are based on the interpretation of the chemical map.*

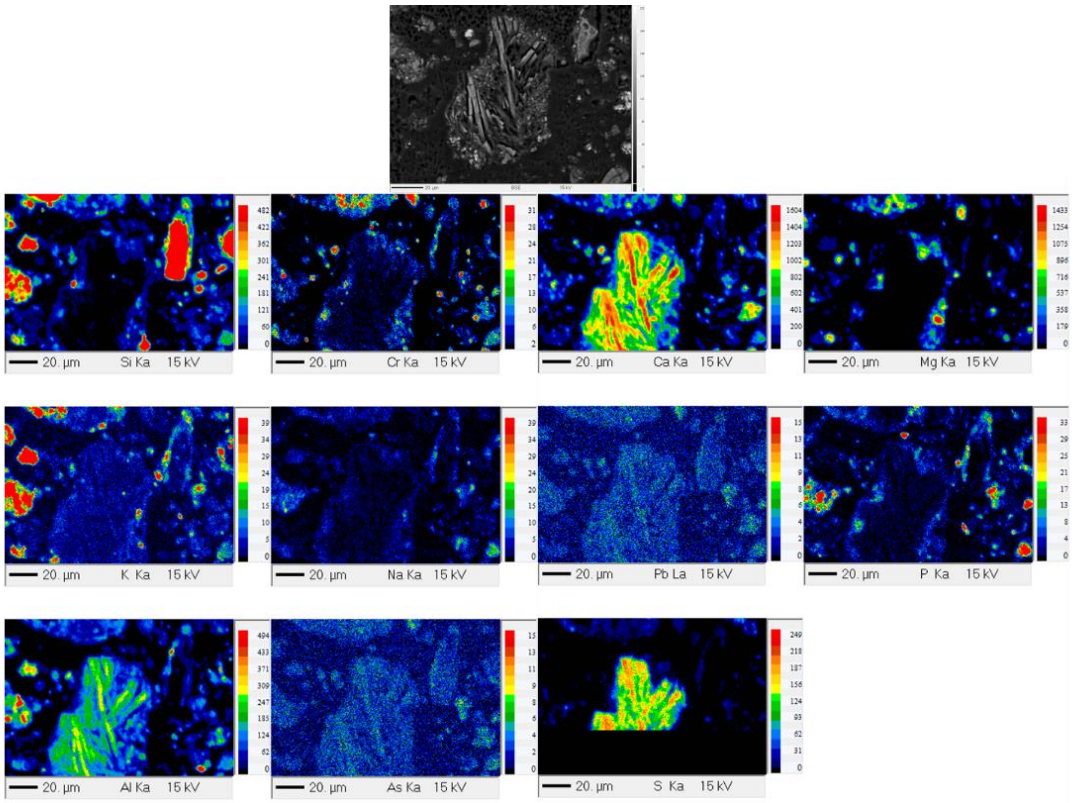

Fig. S4b *Microprobe image of a clump of ettringite particles (top image) and a series of elemental maps on that image. The sample, taken from batch T-RX2 sieved between 15 – 100 um was inserted in a resin and polished. In the upper right quarter, one can see a field dominated by Si, interpreted to be a quartz grain. This grain is coated by microsized particles containing Ca, Cr, K, Mg, Na, Al and P.*

S5] Behaviour of elements during acid leaching experiment

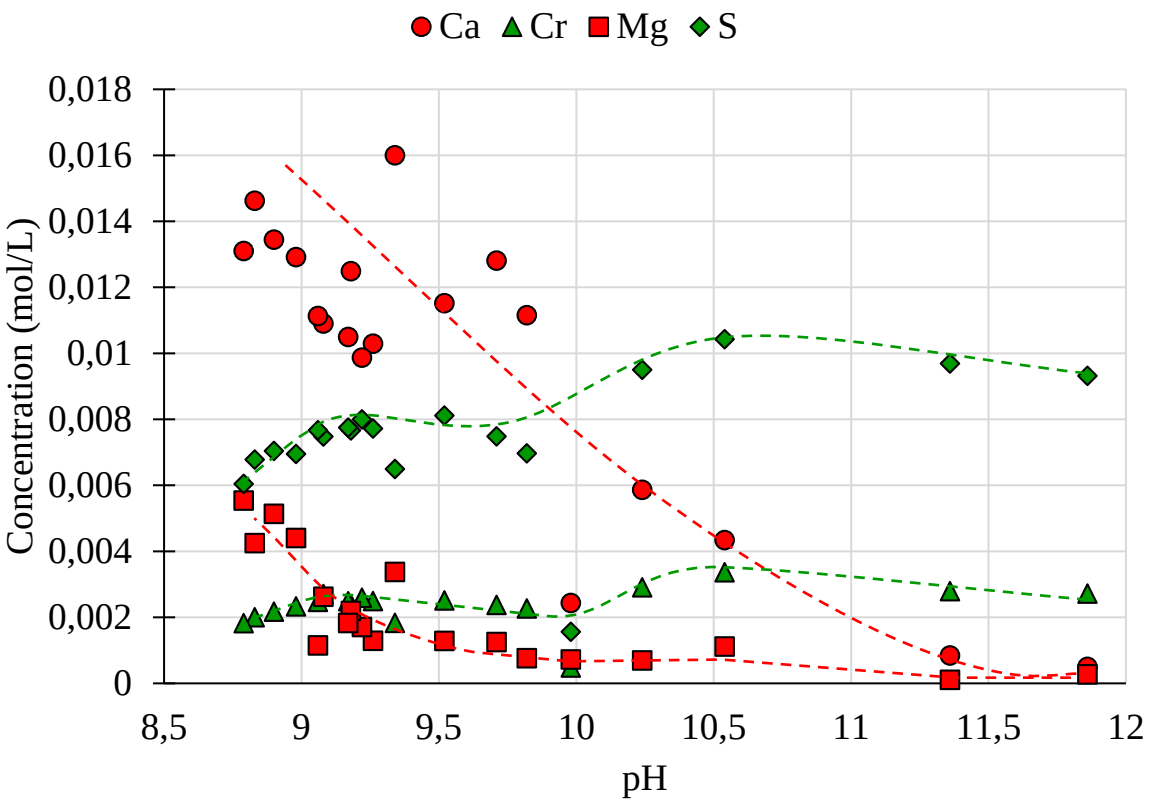

Fig. S5 *Evolution of calcium, chromium, magnesium and sulfur release during the acid leaching experiment. Samples at pH 9.98 and 9.34 are considered as outliers as concentrations of all elements are uncorrelated with respect to their closest neighbours. At pH 9.98 all concentrations are dropping drastically while at pH 9.34 chromium and sulfur concentration are dropping, while calcium and magnesium are increasing. Hand drawn red dotted lines underline calcium and magnesium trends of concentration increase with decreasing pH. Hand drawn green dotted lines underline chromium and sulfur behavior of concentration decrease with decreasing pH.*

In the acid leaching experiment, acidification of the COPR sample in the pH range from 11.86 to 8.79, leads to solubilization. The trends for Ca, Cr, Mg and S, the elements of main interest in this study, are shown in Figure S5. Chromium concentrations were 0.0027 mol/L at pH 11.86 and increased to 0.0034 mol/L at pH 10.54. Then the chromium concentrations decreased progressively to 0.0023 mol/L at pH 9.82. Chromium slightly increased to 0.0025 mol/L at pH 9.26. From this pH to the end of the acidification experiment at pH 8.79, the chromium concentrations decreased progressively down to 0.0018 mol/L. Sulfur concentrations showed the same global trend. First, sulfur concentrations increased from 0.0093 mol/L at pH 11.86 to 0.0104 mol/L at pH 10.54. Then sulfur concentrations decrease to 0.007 mol/L at pH 9.82. An increase of the sulfur concentration to 0.0077 mol/L occured between pH 9.82 and pH 9.26. Finally, sulfur decreased progressively, reaching 0.006 mol/L at pH 8.79. In contrary, trends in calcium and magnesium release (red dotted lines) are similar to those in Geelhoed's work (Geelhoed et al, 2002). As pH descreased, calcium was progressively solubilised, reaching 0.0005 mol/L at pH 11.86 and 0.013 mol/L at pH 8.79. Magnesium solubilisation was recorded starting from pH 9.26, and concentrations reached 0.0055 mol/L at pH 8.79. The trends in chromium and sulfur concentrations were unexpected (green dotted lines). Firstly, no strong release of chromium and sulfur was observed in the pH range between 10.5 and 8.79 where ettringite and hydrocalumite dissolve. Secondly, chromium and sulfur concentrations for the most acidic pH were lower than for initial pH. These observations are different from results obtained by Geelhoed and co-worker (Geelhoed et al, 2002). In their work, chromium and sulfur concentrations increase as pH decreases, reaching a maximum at pH 8.25. Below this pH concentrations decrease to almost zero at pH 4, a phenomenon which was attributed to adsorption on iron oxide phases. In our work, either chromium or sulfur are not solubilised during dissolution of crystalline cement phases, or the stepwise decrease of concentration starting at pH 10.54 is indicative of a sorption or precipitation process starting at that high pH.

S6] Specific sequential extraction protocol

Compared to classical sequential extraction protocols as published in the literature, changes were made to adapt extraction to the specificity of our material (Tab. S3). As the leachable fraction is significant, we modified the protocol to ensure that this fraction is extracted. The standard protocol for leaching, NF EN 12457-2, was included and repeated 3 times to fully extract the easily mobilizable fraction of each element. The reagent used for the exchangeable fraction deviates from the Tessier protocol (Tessier 1979); Na_2SO_4 was selected instead of $MgCl_2$. Indeed, in high pH cement materials such as COPR, ion exchange concerns oxyanions rather than cations. Also, as the focus is put on CrO_4^{2-} mobility, the reagent was selected to favour chromate exchange. Chromate in the cement phase is more easily exchanged by an oxyanion such as sulfate than by a monovalent anion such as chloride (Myneni, 1995). Given that Na^+ and SO_4^{2-} are already present in COPR at relatively high level, their addition as a reagent is not expected to modify mineral equilibria significantly. Reaction time was doubled as desorption kinetics may be slower at elevated pH as in the case of COPR. Carbonate and cement phases are addressed in one single extraction step because conditions for carbonate dissolution (mainly calcite) are overlapping with those forcement phase dissolution. Ettringite, hydrocalumite and hydrogarnet dissolve significantly between pH 11 to 8 (Geelhoed et al, 2002) while the pK_{sp} of $CaCO_3$ is near 8.4 (Ball and Nordstrom, 1991). Based on previous results obtained by Geelhoed on solubility-controlling phases (Geelhoed et al, 2002), we extended the reaction time for the carbonate and cement step from 1 day in the Zeien-Brummer extraction design (Zeien and Brümmer 1989, Elzinga et Cirmo 2010) to 7 days. Solubilization of the carbonate fraction is usually considered as being complete within 24 hours. However, Geelhoed et al. 2002 showed that for COPR, Cr(VI) solubilization was underestimated by up to 20% at 4 days reaction time compared to 27 days. The 7 days reaction time used here is a compromise, ensuring better than 80 % of equilibrium dissolution. For the oxide fraction, reaction time is increased from 2 to 3 hours to best approach complete dissolution of the oxide minerals and full recovery of the elements that were bound to them. Finally, for the residual fraction, lithium borate fusion was preferred to HNO_3 micro-wave digestion or alkaline digestion to make sure of complete dissolution, even of the most recalcitrant particles.

Sequential extraction design	Fractions	Reactive compounds	Operating conditions	Differences and arrangements
Tessier	1. Exchangeable	1M $MgCl_2$ pH 7 (8 mL)	1 h 25°C	
	2. Acid soluble	1M Na-acetate pH 5 (25 mL)	5 h 25°C	
	3. Bound to reducible soil compounds	0.04 M NH_2OH-HCl + 25% (w/v) acid acetic (20 mL)	6 h 96°C	
	4. Bound to oxidizable soil compounds	0.02 M HNO_3 (3 mL) + 30% (w/v) H_2O_2 (5 mL)	2 h 85°C	
		30% (w/v) H_2O_2 (3 mL)	3 h 85°C	
		3.2M NH_4-acetate (5 mL)	0.5 h 25°C	
	5. Residual fraction	Micro-wave HNO_3 digestion	ND	
Zeien-Brummer	1. Carbonate, soluble and mobilizable complexes	1.0 M NH4-acetate pH 6 (25 mL)	24 h 25°C	
	2. Mn(IV)-oxide bound	1 M NH_2OH-HCl (12.5 mL) + 1 M NH_4-acetate (12.5 mL)	0.5 h 25°C	
	3. Organically bound	0.025 M NH_4-EDTA pH 4.6 (25 mL)	1.5 h 25°C	
	4. Weakly cristalline Fe(III) oxides	0.2 M NH_4-oxalate pH 3.25 (25 mL)	2 h 25°C	
	5. Crystalline Fe(III)-oxides	0.1 M ascorbic acid (12.5 mL) + 0.2 M NH_4-oxalate (12.5mL) pH 3.25	2 h 96°C (dark)	
	6. Residual fraction	Micro-wave HNO_3 digestion	ND	
This study	1. Leachable	De-ionized water (standard NF EN 12457-2) (10 mL) (x3 times)	24 h 20-25°C	Extra step not present in previous protocols
	2. Exchangeable	1 M Na_2SO_4 (10 mL)	2 h 20-25°C	Na_2SO_4 instead of $MgCl_2$ for one more hour (Tessier)
	3. Carbonate and cement	1 M NH_4-acetate pH 6 (10 mL) + 50 % (w/v) acetic acid (to maintain pH 6)	168 h (7d) 20-25°C	Seven days instead of 1 day (Zeien-Brummer)
	4. Oxides	0.1 M ascorbic acid (12.5 mL) + 0.2 M NH_4-oxalate (12.5 mL) pH 3.25	3h 96°C	One more hour (Zeien-Brummer)
	5. Residual fraction	Lithium borate fusion + HNO_3	ND (CRPG SARM Nancy)	Fusion instead of digestion

Tab. S6 *Comparison of sequential extraction designs (Tessier and Campbell 1979, Zeien and Brümmer, 1989 in Elzinga and Cirmo, 2010) with the protocol used in this study. ND: no data available. Volumes are for 1 g of material.*

Bibliography

Ball, J.W, et D.K Nordstrom. 1991. Database Wateq4f : User's manual with revised thermodynamic data base and test cases for calculating speciation of major, trace and redox elements in natural waters. Open-File Report 90-129. U.S.G.S.

Elzinga, Evert J., Ashley Cirmo. 2010. « Application of Sequential Extractions and X-Ray Absorption Spectroscopy to Determine the Speciation of Chromium in Northern New Jersey Marsh Soils Developed in Chromite Ore Processing Residue (COPR) ». J. Hazard. Mater. 183 (1-3):145-154.

Geelhoed, Jeanine S., Johannes CL Meeussen, Stephen Hillier, David G. Lumsdon, Rhodri P. Thomas, John G. Farmer, and Edward Paterson. 2002. « Identification and geochemical modeling of processes controlling leaching of Cr (VI) and other major elements from chromite ore processing residue ». Geochim. Cosmochim. Acta 66 (22):3927–3942.

Tessier, A. and P.G.C. Campbell (1979) Sequential extraction procedure for the speciation of particulate trace metals. Anal. Chem. 51 (7):844-851

Myneni, S.C.B. (1995). Oxyanion mineral surface interact ions in alkaline environments: AsO_4 and CrO_4 sorption and desorption in ettringite. Dissertation. The Ohio State University, Colombus, US. 265p.

Zeien, H. and G.W. Brümmer (1989) Chemische Extraktionen zur Bestimmung von schwermetallbindungsformen in Böden. Mitteilgn Dtsch Bodenkundl Gesellsch, 59/I : 505-510.

S7] Pore solution equilibration experiment

The pore solution equilibration experiment is described in the main paper (section "Materials and Methods" and "Results and Discussion" Fig. 7). Here we present the details of data acquired at each sampling step. Only the elements Na, S, Mg, K, Ca and Cr accumulated in relevant concentrations in the leachates and are presented here (figure S7).

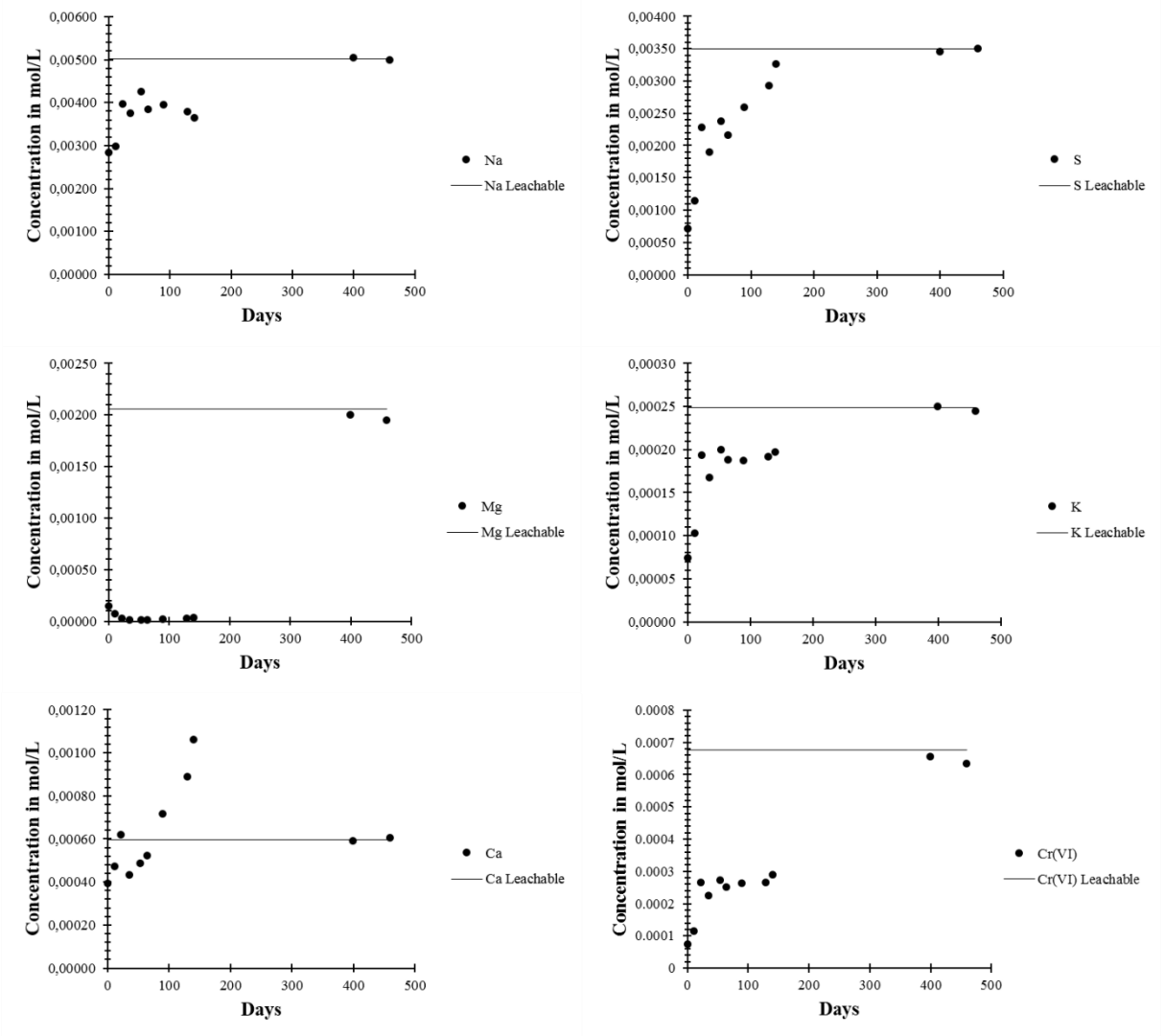

Fig. S7 *Evolution of relevent major element-, sulfur-, and Cr(VI) concentrations in leachate during the pore solution equilibration experiment. Black lines correspond to the concentrations found in the initial leachates performed on the freshly sampled COPR (hereafter the "reference"). The lack of data between 140 and 400 days is related to our initially wrong appreciation of kinetic reactions. Indeed, we initially thought that steady state between solid and pore water had been reached after 140 days, because of the observed relative stability of major element concentrations (except for calcium and sulfur). Thus after 140 days, we stopped doing measurements. Just out of curiosity, a new measurement was done after 400 days, which revealed that all concentrations had evolved, i.e. that they had levelled off close to their initial values. It can be concluded that 400 days is about the time needed to reach true steady state conditions in the material*

Sodium is an easily mobilised element, the concentration at t=0 day, less than 5 minutes after initial leaching was already as high as 2.83 mmol/L. Concentration then raised to 4.3 mmol/L at 53 days and then oscillated between 4.0 and 3.6 mmol/L over the following 90 days until day 140. After 400 days the sodium concentrations had reached 5 mmol/L, close to the initial value of 5.02 mmol/L, and remained stable subsequently. The sulfur showed a nearly constant increase from 0.71 mmol/L to 3.26 mmol/L from 0 to 140 days and a stabilisation near the initial value of 3.5 mmol/L was recorded at 400 days and longer times. As for

sodium, potassium followed the same 2 step trend. Concentrations increased steadily from 0.07 mmol/L to 0.2 mmol/L until 53 days, followed by a relative stabilisation up to 140 days. A second increase occurred between 140 and 400 days, taking the concentrations to 0.25 mmol/L, identical with the initial value. Cr(VI) concentration increased from 0.075 mmol/L at t=0 to 0.26 mmol/L until day 22. Concentration then remained stable up to 140 days and increased between day 140 and 400 to reach 0.65 mmol/L, close to the initial value of 0.68 mmol/L. Calcium behaviour was more irregular. The concentration of calcium was 0.39 mmol/L at t=0 and raised to the value of 0.62 mmol/L in the leachate of the initial extraction at 22 days. Then, a decrease occurred to 0.43 mmol/L at 35 days followed by a nearly constant increase to 1.06 mmol/L at 140 days, exceeding the initial value of 0.6 mmol/L. At 400 days, the calcium concentration had decreased again, reaching the initial leachate concentration and it remained stable close to this value at longer times. Magnesium trends were different from those of the other elements. Magnesium was relatively immobile from the beginning of the experiment to 140 days but it appeared in large amount at 400 days with a concentration near the leachable value and remained at that level at longer times.

The different trends in the solubilisation of compounds suggests that their concentrations depend on a cascade of dissolution, precipitation and maybe adsorption and desorption phenomena. For example, the late solubilisation of magnesium may be due to the presence of the protective concentric mineralogical structure around periclase observed in this work but also in the literature (Hillier et al., 2003). Possibly this layer first had to be destabilised before magnesium could accumulate in solution. Thermodynamic inhibition certainly plays an important role in the heterogeneous COPR material, therefore steady state conditions characterise the material rather than true chemical equilibria.

Cr(VI) dissolution rate

For Cr(VI), a mean dissolution rate k was defined by the following formula :

$k = ([Cr(VI)_{t\ steady\ state}]-[Cr(VI)_{t0}]) \cdot V / (m_{COPR} \cdot \Delta t)$,

where $[Cr(VI)_{t\ steady\ state}]$ and $[Cr(VI)_{t0}]$ are the Cr(VI) concentrations in the leachates at times t0 (leaching test 1 following the initial "reference" leaching within 10 minutes) and time t when steady state was reached (g/L),
V is the volume of water used for the given leaching step (L),
m_{COPR} is the precise mass of the sample aliquote in the given leaching step (kg),
Δt is the time interval between initial sample and the sample at steady state, (day),
k is expressed in g Cr(VI) /kg dry material /day

As steady state was reached in the material during the period between day 140 (initially defined end of experiment) and day 400 (curiosity driven new samplings conduced from day 400 to 460), the dissolution rate cannot be defined precisely. The rate given in the main text corresponds to a minimum value where $t_{steady\ state}$ was set to 400 days.

Bibliography

Hillier, S., M. J. Roe, J. S. Geelhoed, A. R. Fraser, J. G. Farmer, et E. Paterson. 2003. Role of quantitative mineralogical analysis in the investigation of sites contaminated by chromite ore processing residue. *Science of the Total Environment* 308 (1): 195–210.

S8] Estimation of time needed for remediation by natural attenuation

To estimate the time needed for remediation of COPR through natural attenuation by rainfall, we reasoned on a soil column with a base area of 1 m^2 and a depth of 4 m representative of COPR deposits at our site. A schematic is given in figure S8.
The parameters needed to estimate natural attenuation time of COPR at our site are (S8.1.1) the density of COPR, (S8.1.2) the volume to mass ratio needed for total Cr(VI) release, (S8.1.3) the average yearly rainfall, (S8.1.4) the effective precipitation.
We will first describe the acquisition of data (S8.1]) before conducting the calculations (S8.2]).

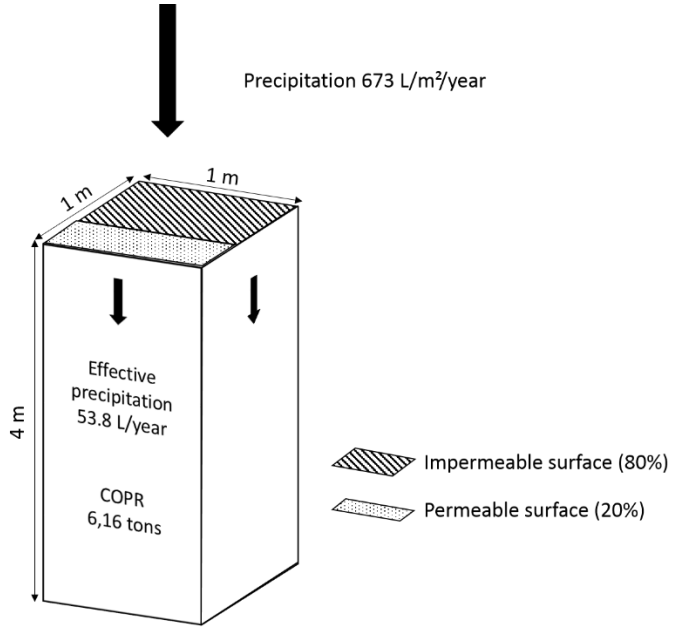

Fig S8 *Illustration of the simplified study site used in our calculation*

S8.1] Methods and Materials

S8.1.1] Density of COPR material by gas pycnometry

For density determination by gas pycnometry, helium is injected in a reference chamber with a volume Vr at a pressure Pr. Then the gas is transferred from the reference chamber to the measurement chamber of volume Vm containing a sample of COPR (mass m) at a measured pressure Pm. The Boyle-Mariotte law is used to determine the volume of the sample (Ve) as below:

$$Ve = Vm - Vr * (\frac{Pr}{Pm} - 1)$$

The density ρ (g/cm3) is then expressed by :

$$\rho = \frac{m}{Ve}$$

S8.1.2] Ratio of water to COPR needed for complete extraction of Cr(VI)

The pore solution equilibration experiment showed that, for 10 grams of COPR, leaching with 100 ml initially extracted 27.4 % of total chromium VI (Fig.7). Supposed that the material reacts in the same way at each pore solution extraction experiment, 3.65 cycles would be needed to extract Cr(VI) completely, corresponding to 365 ml for 10 g of material.

S8.1.3] Average yearly rainfall

We used data from Meteo France at the meteorological station of Lille-Lesquin (https://www.infoclimat.fr). Average annual precipitation, calculated for the period 2000-2019, is 673 L/ m²/year.

S8.1.4] Effective precipitation

Only part of the rain water reaching the surface at the site is expected to infiltrate the COPR deposit. On average 80 % of the surface is sealed due to the presence of infrastructures (Fig. S8). Evapotranspiration reduces the infiltration rate typically to 40 % of total flux. Thus the effective precipitation for our model surface is 53.8 L/year.

S8.2] Results

Pycnometry analyses gave an average density of 2.2 for dry COPR, leading to an estimate of 6.16 tons for our model soil column of 4 m^3, taking into account a porosity of 0.3. The experience on pore solution equilibration (S5) showed by calculation that for 10 grams of COPR, 365 ml of water is needed to achieve complete dissolution of Cr(VI) bearing phases and complete release of that Cr(VI) from the material. Then, by computing total mass of material, volumes of leaching water needed, and effective percolating water, a time of 4179 years is calculated to achieve total Cr(VI) release from COPR by natural attenuation due to rain.

This time estimate is based on back-of-the-envelope calculations using average data on rainfall, a commonly accepted factor for evapotranspiration as well as experimental laboratory data for Cr(VI) release. Thus this duration of natural attenuation should be regarded with a step back, this result only means that natural remediation is a very long process and, if nothing is done, the buried COPR deposit will continue to impact the environment over a time far above the time spans of hundreds of years generally used for predictions on societal and economic evolution.

Bibliography

https://www.infoclimat.fr/climatologie/annee/2018/lille-lesquin/valeurs/07015.html (last consult 2020)